IOP Conference Series: Materials Science and Engineering

PAPER • OPEN ACCESS

Optimization parameters of the heart pump design

To cite this article: V Markučič *et al* 2018 *IOP Conf. Ser.: Mater. Sci. Eng.* **393** 012125

IOP Conf. Series: Materials Science and Engineering **393** (2018) 012125 doi:10.1088/1757-899X/393/1/012125

Optimization parameters of the heart pump design

V Markučič[1], S Krizmanić[1] and F Volarić[1]

[1]University of Zagreb, Faculty of Mechanical Engineering and Naval Architecture, Ivana Lučića 5, 10000 Zagreb, Croatia

E-mail: vedrana.markucic@fsb.hr

Abstract. In this paper, research of optimization parameters of continuous flow heart pump is presented. The application of centrifugal pumps as heart assist devices imposes design limitations on the geometry of the heart pump. Geometry and pump parameters affect the performance and the hemocompatibility of the heart pump. The main quality assessment factor for heart pump is the pump hemocompatibility i.e., the amount of mechanical damage caused by a pump on blood cells. Besides stagnation zones and recirculation zones, wall shear stress is parameter that is used to predict pump hemocompatibility. Second important factor is minimal volume of heart pump with acceptable anatomical fitting. Additional factors are high efficiency and durability. The aim of the research is to propose the optimal design of bladeless centrifugal heart pump. The dimensionless optimization parameters of the heart pump design are derived from Navier - Stokes equation. In conclusion, dimensionless optimization parameters of bladeless centrifugal continuous flow heart pump are presented.

1. Introduction

In recent years, ventricular assist devices (VAD) and total artificial hearts (TAH) had become unrivalled tools for replacing a failed heart. Heart pumps are typically used to bridge the time to heart transplantation, or to permanently replace the heart in case heart transplantation is impossible. Through previous development and implementation, it was observed that pumps with continuous-flow output cause less blood damage and have superior properties than volumetric pumps with pulsating output [1]-[2]. Furthermore, a centrifugal pump is superior to axial flow device [3], [4].

Clinical data showed major complications with infections (80%), thrombosis (19%) and hemorrhagic events (14%). Most hemorrhagic events occurred as a result of antithrombotic therapy. This suggests that influence of heart pump on blood can be significant, hence the hemocompatibility should be priority when designing heart pump. Also, 10% of patients experienced a failure of the device [5]. Reliability, lifetime and bearings also have significant impact on hemocompatibility [6]-[8].

Indicators of hemocompatibility i.e., the amount of mechanical damage of blood cells, are: leukocyte and erythrocyte damage (hemolysis) as well as unwanted platelet activation causing thrombus formation (thrombosis) according to ISO 10993-4 [9], [9].

Numerical and experimental results show increased hemolysis as a direct result of higher shear stresses and longer residence times [4]. Hemolysis was found to increase linearly with exposure time and exponentially with respect to shear stress [11]. The exposure time is increased as a result of stagnation and recirculation zones.

The wall shear stress (WSS) is the parameter that can be used to predict thrombus formation [11], [12]. Generally, thrombus formation occurs when WSS is less than 0.4 Pa [13]-[15].

Besides stagnation and recirculation zones, wall shear stress is main parameter that is used to predict pump hemocompatibility. Further research aims to improve pump design in order to achieve greater hemocompatibility.

2. The design of bladeless centrifugal heart pump

The aim of the research is to propose the design of the bladeless centrifugal heart pump by adaptation of the principles of Tesla pump (Figure 1 and Figure 2). The bladeless centrifugal heart pump creates less shear stress, as the flow is created due to adhesive and cohesive forces, without impact of blood cells on rigid blade surfaces resulting in greater hemocompatibility.

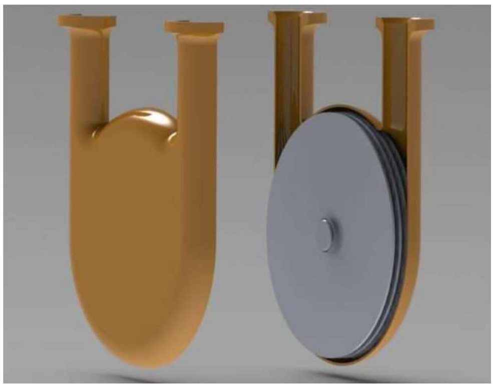

Figure 1. Geometrical model of bladeless centrifugal heart pump [16].

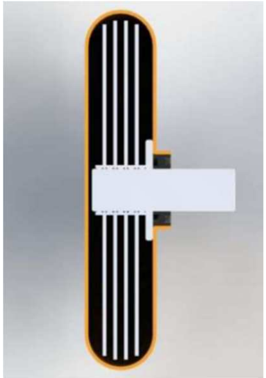

Figure 2. Cross section of bladeless centrifugal heart pump [16].

Research of pump properties is based on applying turbomachinery principles, fluid dynamics theory and dimensional analysis. The influence of design parameters on the pump hemocompatibility is researched. Design parameters are pump head and flow ($\Delta p, Q$), internal and external disc diameter (R_1, R_2), distance of discs (h), and angular velocity (ω).

Essential criteria in heart pump development are pump head and flow. For the essential criteria it is necessary to develop blood pump of acceptable hemocompatibility. Second important factor is minimal volume of heart pump with acceptable anatomical fitting. Additional factors are high efficiency and durability.

3. Optimization parameters

Research of pump properties is based on applying turbomachinery principles, fluid dynamics theory and dimensional analysis on the differential volume of the fluid between two discs (Figure 3). The dimensionless optimization parameters of the heart pump design are derived from the continuity equation and the momentum equation (Navier - Stokes equation).

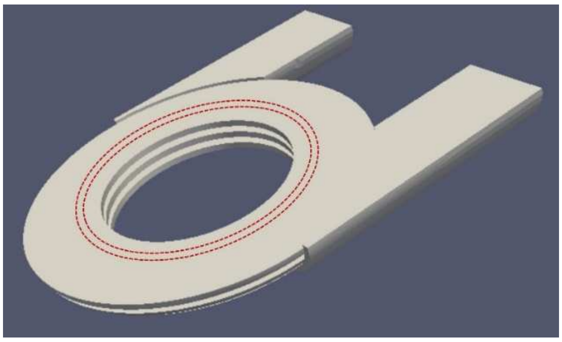

Figure 3. The cylindrical differential volume (red) [16].

IOP Conf. Series: Materials Science and Engineering **393** (2018) 012125 doi:10.1088/1757-899X/393/1/012125

3.1. Cartesian coordinate system

The cylindrical differential volume is fluid volume between two cylindrical discs. The distance of discs is h, also fluid has constant density and dynamic viscosity. The cylindrical differential volume is rectified (Figure 4). The coordinate axis θ correspond to coordinate axis x_1, coordinate axis z correspond to coordinate axis x_2, and coordinate axis r correspond to coordinate axis x_3.

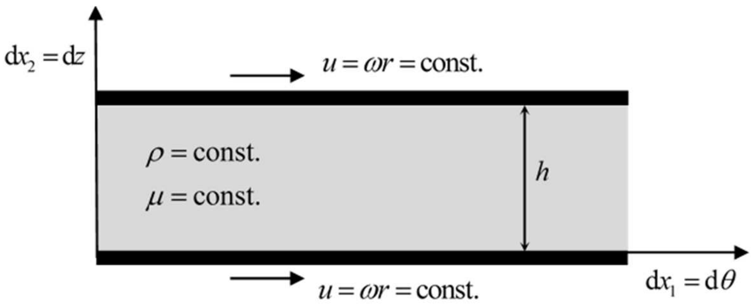

Figure 4. Cartesian coordinate system [17].

The fluid is assumed Newtonian and incompressible. The flow is stationary, planar and laminar with fully developed velocity profile. The effect of gravity is neglected [17], [18].

$$\frac{\partial}{\partial t} \equiv 0, \quad x_3 = \text{const.}, \quad \frac{\partial}{\partial x_3} \equiv 0, \quad v_3 \equiv 0, \quad \frac{\partial v_i}{\partial x_1} \equiv 0, \quad f_i = 0. \tag{1}$$

The laminar flow is described with continuity equation and momentum equation [17], [18]. The continuity equation:

$$\frac{\partial v_j}{\partial x_j} = 0 \tag{2}$$

The equation (1) applied on equation (2) results in $v_2 = C = \text{konst.}$ The momentum equation:

$$\rho \frac{\partial v_i}{\partial t} + \rho v_j \frac{\partial v_i}{\partial x_j} = -\frac{\partial p}{\partial x_i} + \mu \frac{\partial^2 v_i}{\partial x_j \partial x_j} + \rho f_i \tag{3}$$

The equation (1) applied on equation (3) results in:

$$i = 1, \qquad \frac{\partial p}{\partial x_1} = \mu \frac{\partial^2 v_1}{\partial {x_2}^2} \tag{4}$$

$$i = 2, \qquad \frac{\partial p}{\partial x_2} = 0 \tag{5}$$

$$i = 3, \qquad \frac{\partial p}{\partial x_3} = 0 \tag{6}$$

The equation (4) further develops in:

$$\underbrace{\frac{dp}{dx_1}}_{f(x_1)} = \mu \underbrace{\frac{d^2 v_1}{dx_2^2}}_{f(x_2)} = \text{konst.} \tag{7}$$

After second derivation and implementation of boundary conditions $x_2 = 0, v_1 = u$ and $x_2 = h, v_1 = u$, equation (7) becomes:

$$v_1(x_2) = \frac{1}{2\mu}\frac{\mathrm{d}p}{\mathrm{d}x_1}\cdot\left[x_2{}^2 - h\cdot x_2\right] + u \tag{8}$$

The equation (8) shows that velocity is a function of angular velocity and radius, $v_1 = f(u) = f(\omega r)$. Therefore, it is necessary to observe the above mentioned problem in the cylindrical coordinate system.

3.2. Cylindrical coordinate system

It is impossible to exactly solve fluid flow in cylindrical coordinate system (Figure 5), so the velocity profile from the equation (8) is obtained. The application of equation (9) on Navier-Stokes equation in cylindrical coordinates is acceptable approximation [18]. The velocity profile in the cylindrical coordinate system:

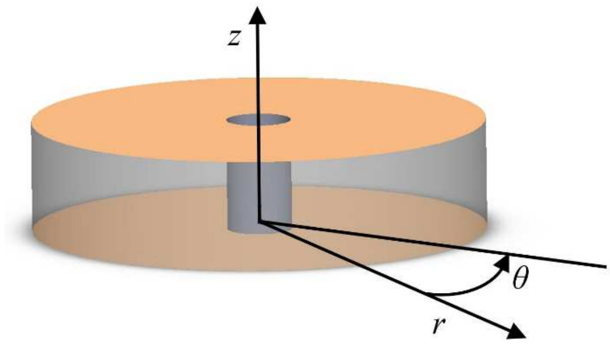

Figure 5. The cylindrical coordinate system of the differential volume [18].

$$v_\theta(z) = \frac{1}{2\mu}\frac{\mathrm{d}p}{\mathrm{d}\theta}\cdot\left[z^2 - h\cdot z\right] + \omega r \tag{9}$$

The wall shear stress (WSS) is the parameter that can be used to predict thrombus formation. The wall shear stress in cylindrical coordinate system is:

$$\tau_{\theta z} = \mu\left(\frac{\partial v_\theta}{\partial z} + \frac{1}{r}\frac{\partial v_z}{\partial \theta}\right) \tag{10}$$

The equation (10) is further solved:

$$\tau_{\theta z} = \frac{1}{2}\frac{dp}{d\theta}(2z - h) \tag{11}$$

The equation (11) can be simplified with next expression:

$$\frac{dp}{d\theta} = \frac{\Delta p}{2r\pi} \tag{12}$$

Finally, the wall shear stress is shown with next expression:

$$\tau_{\theta z} = \frac{\Delta p}{4r\pi}(2z - h) \tag{13}$$

The wall shear stress have maximum and minimum quantity on the surface of the discs ($z = 0,\ z = h$).

$$\left(\tau_{\theta z}\right)_{\min/\max} = \pm \frac{\Delta p \cdot h}{4r\pi} \tag{14}$$

The other important factor is pump flow. The pump flow in cylindrical coordinate system is defined with:

$$Q = \int_{R_1}^{R_2}\int_{0}^{h} v_\theta \cdot \mathrm{d}z \cdot \mathrm{d}r \tag{15}$$

After solving double integral in equation (15), pump flow is derived:

$$Q = \frac{1}{2\mu}\frac{\Delta p}{2\pi}\left(-\frac{h^3}{6}\right)\cdot \ln\left(\frac{R_2}{R_1}\right) + \frac{\omega h R_1^2}{2}\left(R_2^2 - R_1^2\right) \tag{16}$$

3.3. The dimensionless optimization parameters

The pump flow equation (16) can further be rearranged [19]. The second part is divided with R_1^2, and then the whole equation can be multiplied with $\frac{\omega h R_1^2}{2}$, resulting in:

$$2\frac{Q}{\omega h R_1^2} = \frac{-1}{12\pi}\frac{\Delta p \cdot h^2}{\mu \omega R_1^2}\cdot \ln\left(\frac{R_2}{R_1}\right) + \left(\frac{R_2^2}{R_1^2} - 1\right) \tag{17}$$

The Reynolds number is:

$$\mathrm{Re} = \frac{\rho \cdot \omega R_1 \cdot h}{\mu} \tag{18}$$

The Reynolds number formula is implemented in equation (17):

$$2\frac{Q}{\omega h R_1^2} = \frac{-1}{12\pi}\frac{\Delta p \cdot h^2}{\rho \omega^2 R_1^3}\cdot \mathrm{Re}\cdot \ln\left(\frac{R_2}{R_1}\right) + \left(\frac{R_2^2}{R_1^2} - 1\right) \tag{19}$$

The equation (19) can be further rearranged in dimensionless form [9]:

$$2 \cdot \Pi_Q = \frac{-1}{12\pi}\cdot \Pi_p \cdot \mathrm{Re}\cdot \ln\left(\Pi_R\right) + \left(\Pi_R^2 - 1\right) \tag{20}$$

In equation (20), dimensionless optimization parameters are:

$$\Pi_Q = \frac{Q}{\omega h R_1^2} \tag{21}$$

$$\Pi_p = \frac{\Delta p \cdot h^2}{\rho \omega^2 R_1^3} \tag{22}$$

$$\Pi_R = \frac{R_2}{R_1} \tag{23}$$

In the turbomachinery theory it is normal that dimensionless parameter of pressure is a function of other dimensionless parameters, the equation (20) is further rearranged in following manner:

$$\Pi_p = 12\pi \cdot \frac{\left(\Pi_R^2 - 1\right) - 2\cdot \Pi_Q}{\mathrm{Re}\cdot \ln\left(\Pi_R\right)} \tag{24}$$

Furthermore, the equation (13) that shows final form of the wall shear stress can also be displayed in dimensionless form:

$$\Pi_\tau = \frac{\tau_{\theta z} \cdot 4r\pi}{\Delta p \cdot (2z - h)} \tag{25}$$

4. Conclusion

The dimensionless optimization parameters of bladeless centrifugal continuous flow heart pump are presented:

- dimensionless pump flow parameter:

$$\Pi_Q = \frac{Q}{\omega h R_1^2} \tag{26}$$

- dimensionless pump head parameter:

$$\Pi_p = \frac{\Delta p \cdot h^2}{\rho \omega^2 R_1^3} \tag{27}$$

- dimensionless radius (geometry) parameter:

$$\Pi_R = \frac{R_2}{R_1} \tag{28}$$

- dimensionless wall shear stress parameter:

$$\Pi_\tau = \frac{\tau_{\theta z} \cdot 4r\pi}{\Delta p \cdot (2z - h)} \tag{29}$$

The essential criteria are pump head and flow ($\Delta p, Q$) which are defined with exact values. Furthermore, the value range of the wall shear stress with acceptable hemocompatibility is also defined.

The rest of design parameters: internal and external disc diameter (R_1, R_2), distance of discs (h), and angular velocity (ω) have to be determined. The unknown values of design parameters (R_1, R_2, h, ω) have to be determined in a way to fulfil constrains of the dimensionless optimization parameters with respect to minimal volume of the heart pump.

References

[1] Fujii Y, Ferro G, Kagawa H, Centola L, Zhu L, Ferrier W T, Talken L, Riemer R K, Maeda K, Nasirov T, Hodges B, Amirriazi S, Lee E, Sheff D, May, J, May R and Reinhartz O 2015 Is Continuous-flow Superior to Pulsatile Flow in Single Ventricle Mechanical Support? Results from a Large Animal Pilot Study, *Asaio Journal* **61**(4) 443-449

[2] Cohn W E, Timms D L and Frazier O H 2015 Total Artificial Hearts: Past, Present, and Future, *Nature Reviews Cardiology* **12**(10) 609-625

[3] Pirbodaghi T, Cotter C and Bourque K 2014 Power Consumption of Rotary Blood Pumps: Pulsatile Versus Constant-Speed Mode, *Artificial Organs* **38**(12) 1024-1033

[4] Schibilsky D, Lenglinger M, Avci-Adali M, Haller C, Walker T, Wendel H P and Schensak C 2015 Hemocompatibility of Axial Versus Centrifugal Pump Technology in Mechanical Circulatory Support Devices, *Artificial Organs* **39**(8) 723-730

[5] Fraser K H, Zhang T, Taskin M E, Griffith B P and Wu Z J 2012 A Quantitative Comparison of Mechanical Blood Damage Parameters in Rotary Ventricular Assist Devices: Shear Stress, Exposure Time and Hemolysis Index, *Journal of Biomechanical Engineering-Transactions of the ASME* **134**(8) 11

[6] Torregrossa G, Morshuis M, Varghese R, Hosseinian L, Vida V, Tarzia V, Loforte A, Duveau D, Arabia F, Leprince P, Kasirajan V, Beversdoft F, Musumeci F, Hetzer R, Krabatsch T, Gummert J, Copeland J and Gerosa G 2014 Results with Syncardia Total Artificial Heart Beyond 1 Year, *Asaio Journal* **60**(6) 626-659

[7] Amaral F, Gross-Hardt S, Timms D, Egger C, Steinseifer U and Schmitz-Rode T 2013 The Spiral Groove Bearing as a Mechanism for Enhancing the Secondary Flow in a Centrifugal Rotary Blood Pump, *Artificial Organs* **37**(10) 866-939

[8] Amaral F, Egger C, Steinseifer U and Schmitz-Rode T 2013 Differences Between Blood and a Newtonian Fluid on the Performance of a Hydrodynamic Bearing for Rotary Blood Pumps, *Artificial Organs* **37**(9) 786-877

[9] da Silva B U, Jatene A D, Leme J, Fonseca J W, Silva C, Uebelhart B, Suzuku C K and Andrade A J 2013 In Vitro Assessment of the Apico Aortic Blood Pump: Anatomical Positioning, Hydrodynamic Performance, Hemolysis Studies, and Analysis in a Hybrid Cardiovascular Simulator, *Artificial Organs* **37**(11) 950-952

[10] Seyfert U T, Biehl V and Schenk J 2002 In Vitro Hemocompatibility Testing of Biomaterials According to the ISO 10993-4, *Biomolecular Engineering* **19**(2-6) 91-95

[11] Boehning F, Mejia T, Schmitz-Rode T and Steinseifer U 2014 Hemolysis in a Laminar Flow-Through Couette Shearing Device: An Experimental Study, *Artificial Organs* **38**(9) 761-765

[12] Basciano C, Kleinstreuer C, Hyun S and Finol E A 2011 A Relation Between Near-Wall Particle-Hemodynamics and Onset of Thrombus Formation in Abdominal Aortic Aneurysms, *Annals of Biomedical Engineering* **39**(7) 2010-2035

[13] Di Achille P, Tellides G, Figueroa C A and Humphrey J D 2014 A Haemodynamic Predictor of Intraluminal Thrombus Formation in Abdominal Aortic Aneurysms, *Proceedings of the Royal Society A* **470** 20140163-1–20140163-22

[14] Zambrano B A, Gharahi H, Lim C, Jaberi F A, Choi J, Lee W and Baek S 2015 Association of Intraluminal Thrombus, Hemodynamic Forces, and Abdominal Aortic Aneurysm Expansion Using Longitudinal CT Images, *Annals of Biomedical Engineering* **44**(5) 1502-1515

[15] Klodell C T, Massey H T, Adamson R M, Dean D A, Horstmanshof D A, Ransom J M, Salerno C T, Cowger J A, Aranda J M Jr, Chen L, Long J W and Dembitsky W 2015 Factors Related to Pump Thrombosis with the Heartmate II Left Ventricular Assist Device, *Journal of Cardiac Surgery* **30**(10) 775-854

[16] Pagani F D 2016 Continuous-Flow Left Ventricular Assist Device Thrombosis: A Solvable Problem, *Asaio Journal* **62**(1) 3-5

[17] Horvat M 2015 *Heart Pimp h-Q Characteristic Calculation*, Faculty of Mechanical Engineering and Naval Architecture, University of Zagreb, BSc Thesis

[18] Virag Z, Šavar M and Džijan I 2017 *Mehanika fluida II*, Faculty of Mechanical Engineering and Naval Architecture, Manualia Universitatis studiorum Zagrabiensis

[19] Schobeiri M T 2010 *Fluid Mechanics for Engineers*, Springer-Verlag Berlin Heidelberg

[20] Gibbings J C 2011 *Dimensional Analysis*, Springer Science & Business Media